Surface layering properties of Intralipid phantoms

Nico Bodenschatz,[1, a)] Philipp Krauter,[1] Florian Foschum,[1] Steffen Nothelfer,[1] André Liemert,[1] Emanuel Simon,[1] Sabrina Kröner,[1] and Alwin Kienle[1]

Institut für Lasertechnologien in der Medizin und Meßtechnik, Helmholtzstr. 12, D-89081 Ulm, Germany

(Dated: 27 March 2015)

Intralipid has become an extensively studied and widely used reference and calibration phantom for diffuse optical imaging technologies. In this study we call attention to the layering properties of Intralipid emulsions, which are commonly assumed to have homogeneous optical properties. By measurement of spatial frequency domain reflectance in combination with an analytical solution of the radiative transfer equation for two-layered media, we make quantitative investigations on the formation of a surface layer on different dilutions of Intralipid. Our findings are verified by an independent spatially resolved reflectance setup giving evidence of a time dependent, thin and highly scattering surface layer on top of Intralipid-water emulsions. This layer should be considered when using Intralipid as an optical calibration or reference phantom.

I. INTRODUCTION

Most diffuse optical technologies make use of reference and calibration phantoms for quantification of absorption and scattering properties in turbid media[1]. One of the most frequently used diffuse optical phantoms is Intralipid (Fresenius Kabi AG, Germany), which has also become one of the most extensively studied reference materials in the biomedical optics community[1–15]. Along with general investigations on its optical properties[2–5], Intralipid has been subject to the research on dependent scattering at high concentrations of scatterers[5–8] and the particle size and shape distribution of scatterers has been quantified together with corresponding scattering phase functions[2,9,10]. Furthermore, the possibility to modify the scattering characteristics of Intralipid using optical clearing agents was studied[11]. Recently, also the stability and variability of Intralipid and its temperature dependent optical properties were analyzed[12,15]. In this context, also the batch to batch variation of numerous Intralipid samples[13] and its micro physical stability subject to the dilution with water[7] were investigated.

These studies underline the significance of a well defined reference and calibration material for diffuse optical technologies. With our work, we seek to contribute to this research on Intralipid and report on the dynamic formation of a thin layer with comparatively high scattering on the surface of Intralipid emulsions. Especially in combination with an absorbing agent, this surface layer is even visible to the naked eye in the form of flow marks when gently stirring the emulsion after several minutes of standstill. In Figure 1, we show a photograph of an Intralipid phantom, which has been diluted with distilled water and mixed with a small amount of ink. Fifteen minutes after mixing of the emulsion, a surface film can be made visible by gentle stirring of the surface. Without addition of an absorber or at early times after mixing, this surface layer is also existent, yet barely visible to the eye. Therefore, our studies focus on the formation of this layer over time for different dilutions of Intralipid. In this context, we also seek to quantify the error related to this surface effect when using Intralipid as a reference or calibration phantom.

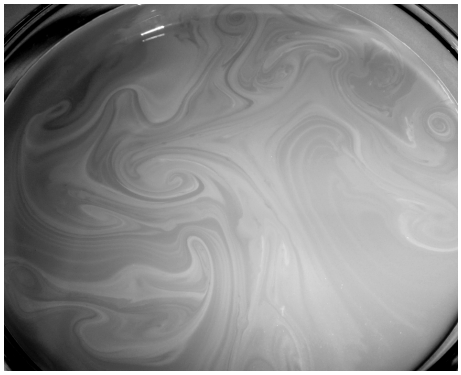

FIG. 1. Macroscopic visibility of the surface layer on a water-Intralipid-ink dilution ($\mu_a \approx 0.3\,\mathrm{mm}^{-1}$ and $\mu_s' \approx 3\,\mathrm{mm}^{-1}$) captured after 15 minutes of standstill and subsequent gentle stirring. This camera image is enhanced in contrast to improve the visibility of the flow marks.

Our experimental studies make use of spatial frequency domain imaging (SFDI), which is an established diffuse optical imaging technique that is frequently applied to probe absorption and scattering properties of turbid media by projection of spatially modulated sinusoidal light intensity patterns[16–21]. We combine this technique with an analytical solution to the radiative transfer equation (RTE) for layered media. The derivation of this model corresponds to that of the semi-infinite non-layered case and will be published soon[22,23]. The model is validated with Monte Carlo simulations and shows excellent agreement with simulations for layered media with layer-specific optical properties and therefore renders the optical characterization of the Intralipid surface layer possible[24].

In Section II we provide detailed information on our experimental SFDI setup along with the measurement

[a)] nico.bodenschatz@ilm.uni-ulm.de

and evaluation protocol. Subsequently, our experimental findings are presented in Section III together with quantitative results on the surface layer properties. Based on the thickness and the relative scattering intensity of the surface layer, we then assess the typical error related to the Intralipid inhomogeneity in SFDI (Section IV) and name possible causes of the surface effect. In Section V, we confirm the experimental findings obtained in the spatial frequency domain by also measuring the spatially resolved reflectance using point like illumination of Intralipid. Finally, we conclude on the impact of the surface effect for different measurement modalities.

II. MATERIALS AND METHODS

All our analysis is based on a single batch of Intralipid 20 % (Fresenius Kabi, 2014), even though we observe the layering effect throughout various batches. In order to achieve maximum precision, the scattering phase function of this specific batch was previously determined by single scattering experiments in a separate goniometer setup[25]. The experimental phase function data is subsequently used in our analytical evaluation model. Accurate modeling with this phase function is only valid for sufficiently high dilutions of Intralipid with negligible dependent scattering effects. Based on previous analysis of dependent scattering in Intralipid[8], we only consider emulsions with a volume concentration of scatterers below 5 %. This corresponds to Intralipid emulsions with reduced scattering $\mu_s' \leq 6\,\mathrm{mm}^{-1}$.

Our quantitative analysis of Intralipid is carried out using a SFDI setup with a halogen light source in combination with a bandpass filter with transmission maximum at $\lambda = 600\,\mathrm{nm}$ and FWHM of 10 nm (note, that the same wavelength is used for the previously mentioned goniometric studies). Spatial frequency patterns are produced by a digital mirror device (DMD - V4100 board with 0.7" XGA, Vialux, Germany) and the reflectance is captured by a CCD camera (QSI 640, Quantum Scientific Imaging, Mississippi, USA) with a $38\,\mathrm{mm} \times 38\,\mathrm{mm}$ field of view.

SFDI is performed at 16 different spatial frequencies between $0\,\mathrm{mm}^{-1} \leq f \leq 2.7\,\mathrm{mm}^{-1}$. The large number of spatial frequencies employed is not a prerequisite for our experimental investigation, but provides additional stability to the fit process. Very high spatial frequencies are projected to increase the surface sensitivity of the technique for enhanced quantification of the Intralipid surface layer properties. In this spatial frequency regime, correction of the measured spatial frequency domain (SFD) reflectance values is necessary to account for defocussing and aberration in the projected SFD pattern. We consider these height dependent effects by measurement of the projected amplitude using a reflecting anodized piece of aluminum showing practically no volume scattering.

The required precision in sample height positioning is guaranteed by a confocal height detector (IFS2400, Micro-Epsilon, Germany) to a precision of 50 µm. Optical height detection requires a sufficiently large backscattering signal and therefore our study had to be limited to $\mu_s' = 2\,\mathrm{mm}^{-1}$ as the lowest possible scattering value. Experimental data is averaged and evaluated only for a circular area of diameter 15 mm in the center of the measuring vessel at the site of height measurement. The formation of a meniscus of the liquid is minimized by completely filling the vessel which is 9 cm in diameter.

For this study, five different dilutions of Intralipid are prepared by addition of different amounts of double distilled water (20 °C). The pure Intralipid 20 % is stored in a fridge (at 6 °C) and diluted to five different volume concentrations (7 %, 11 %, 15 %, 19 % and 23 %) to obtain reduced scattering properties in the range $2\,\mathrm{mm}^{-1} \leq \mu_s' \leq 6\,\mathrm{mm}^{-1}$ at $\lambda = 600\,\mathrm{nm}$. Note, that the absolute volume concentration of scatterers is 0.2 times the stated 'Intralipid 20 %' volume concentration.

The time between preparation and measurement of Intralipid is about 30 min. During this time and all subsequent measurements, samples are kept at room temperature (20 °C). Each dilution of Intralipid is repeatedly measured over a duration of one hour, with a measurement interval of four minutes. The emulsion is stirred only once, shortly before being filled into the measuring vessel. After settling of the surface motion, the sample height is precisely adjusted producing a time delay of two minutes between stirring of the emulsion and first measurement. During the subsequent series of repeated measuring, the Intralipid dilution is not stirred any further and the sample height is adjusted every eight minutes in order to account for evaporation induced changes in height. Without readjustment of the sample height, a small drift in the experimental data due to defocussing effects would be noticeable after about 30 min.

For consideration of the projected light intensity and camera sensitivity, reference frames are captured on a spectralon (Labsphere, USA) reflectance standard in advance. This calibration renders the measurement of absolute SFD reflectance values possible and requires the capture of only one intensity reference at spatial frequency $f = 0\,\mathrm{mm}^{-1}$ with the DMD set to homogeneous projection. We do not make use of crossed linear polarizers for suppression of specular surface reflection. Instead, we employ oblique projection of spatial frequencies at the angle of incidence $\theta = 35°$ and position the camera, with numerical aperture of $\mathrm{NA} = 0.025$, uprightly above the sample.

Evaluation of the experimental data is based on a trust-region-reflective fit algorithm using our analytical solution to the RTE for two layered media. Even though this solution allows for arbitrary orders of precision to be calculated, we limit the order of spherical harmonics expansion to $l = 9$ for reasons of computation time. In our case, however, higher orders of computation produce an insignificant change to the evaluation results. The analytical model used for this study assumes and infinitely thick second layer and both layers to have different scattering coefficients. For both layers, our model makes use

of the experimentally determined scattering phase function of Intralipid. The evaluation algorithm fits four parameters to our experimental data, namely the reduced scattering $\mu_s'(1)$ and $\mu_s'(2)$ of the first and second layer, respectively, the thickness d of the first layer and the absorption coefficient μ_a. The investigated surface layer is very thin and due to the weak intrinsic absorption of Intralipid, our measurements are insensitive to the absorption $\mu_a(1)$ in the first (upper) layer. Therefore, we set $\mu_a = \mu_a(1) = \mu_a(2)$ in the evaluation model. Furthermore, our experiments have only small sensitivity to the separate determination of both $\mu_s'(1)$ and d. According to our model, an increase of $\mu_s'(1)$ can be largely compensated by a decrease in d in the fit process for small layer thicknesses. Therefore, a normalized effective layer thickness $[\mu_s'(1) - \mu_s'(2)] \cdot d$ will be examined in Section III.
Our measurements are also performed on highly absorbing Intralipid emulsions by use of Ink as an added absorbing agent. High absorption brings the benefit of increased surface sensitivity for diffuse optical investigations. Almost the same surface layer properties could be obtained for phantoms with added absorber. However, the addition of ink increases the inhomogeneity of the Intralipid optical properties since ink seems to not equally penetrate the surface layer. This can be observed by visual inspection of an apparent separation of oil droplets and the ink-water dilution leading to surface flow marks (see Fig. 1). Due to slow movements of the surface film based on natural air circulation, the measurement is impaired by the temporal and lateral variation of the optical properties. For this reason, we present data only for pure Intralipid-water emulsions without additional absorber and average our experimental data over a circular area of diameter 15 mm.

III. EXPERIMENTAL RESULTS

Even without usage of our evaluation model, the qualitative change of Intralipid optical properties can be observed from our SFD reflectance data. Figure 2 shows 15 measured SFD reflectance curves versus spatial frequency for one dilution of Intralipid ($\mu_s' = (2.9 \pm 0.1)\,\mathrm{mm}^{-1}$). These curves correspond to a time series captured over a duration of one hour in intervals of four minutes. As indicated by the arrow, an increase in SFD reflectance with time can be observed especially for high spatial frequencies. In SFDI, high spatial frequencies are more sensitive to shallow light propagation and thus small penetration depths. Since the Intralipid sample is not modified between subsequent iterations (no stirring), the rise of the reflectance curves is directly related to the change in the optical properties of the Intralipid surface. We make the important finding, that stirring of the Intralipid sample after a measurement series of one hour brings the emulsion back to its initial optical properties. This conclusion is based on a second time series after stirring of the sample, in which almost identical reflectance curves are

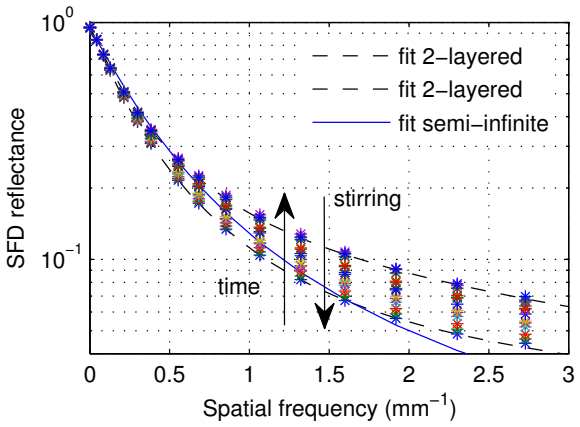

FIG. 2. SFD reflectance of diluted Intralipid with $\mu_s'(2) \approx 3\,\mathrm{mm}^{-1}$ for iterative measurements over a duration of one hour. The arrows indicate the rise in SFD reflectance with time and the reversibility of the process by stirring. The dashed curves present fit results to the first and last data series using our two-layer RTE model. The solid curve gives the rather poor fit result of a semi-infinite model to the first data series and visualizes the impact of the Intralipid surface layer.

obtained as in the first series.
In Figure 2 the dashed curves give a fit of our two layered model to the first and last data curve and thereby indicate the very good agreement between our analytical model and the measured reflectance data. Furthermore, we also display a second fit to the first data curve using a corresponding RTE model which assumes the sample optical properties to be non-layered and homogeneous. The poor match of this fit states another indicator of the Intralipid inhomogeneity.
All data curves shown in Figure 2 and that of all other four Intralipid dilutions are evaluated by our two-layer RTE model. For some data curves, variability in the fit results is obtained in $\mu_s'(1)$ and d when using different start values of the fit variables. This demonstrates the method's weakness in separating these two parameters having very similar influence on the reflectance curve. Therefore, we analyze a normalized effective optical layer thickness, which we define by $[\mu_s'(1) - \mu_s'(2)] \cdot d$ and which is independent of the selected start parameters. Figure 3 displays this effective layer thickness over time for five different Intralipid dilutions. It can be observed that the effective layer thickness rises with time for all dilutions with an offset of about 0.1 at time zero. This offset could, for example, be due to a 10 µm thick surface layer with the reduced scattering increased by $\Delta\mu_s' = \mu_s'(1) - \mu_s'(2) = 10\,\mathrm{mm}^{-1}$. The effective layer thickness of Intralipid seems to have some dependence on the Intralipid concentration c.
Despite the relatively weak absolute sensitivity to the layer thickness d (independent of $\mu_s'(1)$), our evaluation results of all Intralipid dilutions suggest a very similar

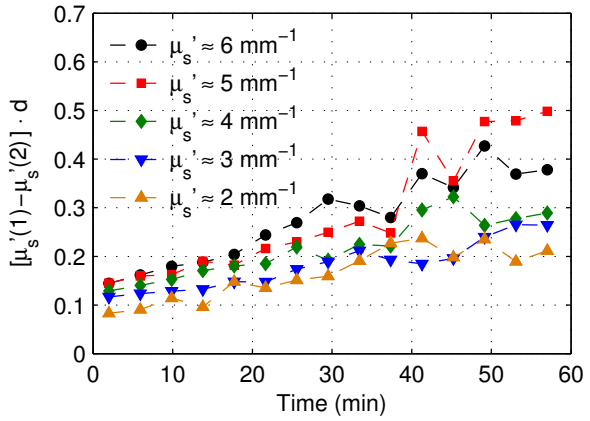

FIG. 3. Effective surface layer thickness of different Intralipid dilutions over time, as obtained by fitting of the RTE model to experimental data. The effective layer thickness is calculated using the fit results for $\mu_s'(1)$, $\mu_s'(2)$ and d.

increase in d from about $d = 6 \pm 3\,\mu\text{m}$ at the initial time step to $d = 60 \pm 30\,\mu\text{m}$ after one hour. At the same time, a decrease in $\mu_s'(1)$ with time is observed for all five Intralipid dilutions.

During every experimental time series, we observe progressive lateral inhomogeneity of the Intralipid optical properties due to natural air circulation induced flow. This produces an increasing instability in the effective layer thickness (as given in Fig. 3) for times above 30 min. We partly compensate for this effect by averaging of the SFD reflectance in each measurement over a circular area of diameter 15 mm.

Furthermore, we observe that the experimentally derived reduced scattering $\mu_s'(2)$ of the assumed semi-infinite bottom layer shows an increase over time between 2 % (strongest dilution of Intralipid) and 11 % (most concentrated dilution) and contributes to the temporal variation of optical properties. We ascribe this effect to the approximate nature of our two-layer evaluation model, rather than to a real change of optical properties deeply below the surface. In this regard, we assume the actual optical properties of Intralipid to vary gradually with depth near the surface, rather than having a distinct two-layer profile.

Moreover, also the obtained fit results for μ_a show a time dependence for some of the measured Intralipid samples. In absolute terms, however, this dependence is very small since the derivation of absorption values relates to the low spatial frequency regime and therefore has only small surface sensitivity. Nevertheless, the interdependence of μ_s' and μ_a in the fit process can propagate errors and cause relative inaccuracies in μ_a of more than 50 % in the low absorption regime ($\mu_a \approx 1 \cdot 10^{-4}\,\text{mm}^{-1}$). Even without error propagation, major inaccuracies in μ_a occur for wavelengths above $\lambda = 1300\,\text{nm}$, where the very high water absorption produces a strong surface sensitivity even at spatial frequency zero (total reflectance configuration). According to additional measurements and simulations, this can give rise to errors in μ_a of more than 35 %.

IV. DISCUSSION

Our experimental results suggest a significant deviation from the commonly assumed homogeneity on the surface of Intralipid samples. The effective surface layer thickness presented in Figure 3 is a quantitative measure of the Intralipid inhomogeneity and can be used to assess the error for Intralipid as a reference material. However, the actual error due to layering of Intralipid for a specific measurement setup is strongly dependent on the measuring modality. For example, in SFDI, the spatial frequency range implicates the degree of surface sensitivity and therefore governs the impact of the Intralipid surface layer on measurement results.

In the following, we seek to quantify a typical error in μ_s' related to the layering of Intralipid. In doing so, the scattering value of trust for every Intralipid dilution needs to be identified in a first step. Since layering evolves with time, we assume the first measurement after stirring to yield the most reliable value of the reduced scattering of Intralipid. Therefore, we make the assumption that $\mu_s'(2)$ at time zero obtained from the two-layer fit is the true scattering value for every phantom. In a second step, our experimental data is once again evaluated using a similar analytical model which does not take into account a surface layer, but assumes a semi-infinite geometry. The reduced scattering value obtained in this way deviates from the previously defined value of trust and its relative deviation is presented in Figure 4 for all five dilutions of Intralipid. For calculation of the relative error

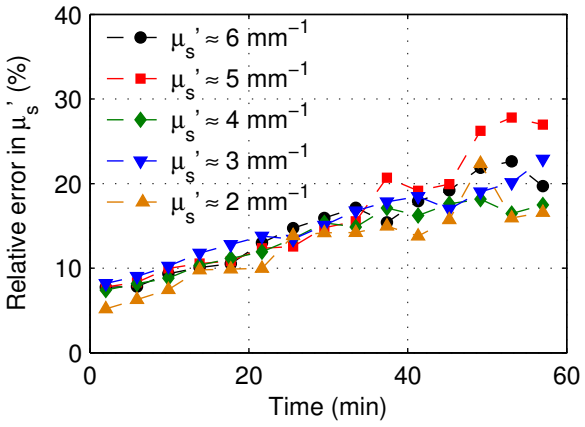

FIG. 4. Relative error in μ_s' for the use of Intralipid as a reference material, quantifying the deviation in μ_s', if the layering effect is not considered in the evaluation theory.

in μ_s' only two spatial frequencies, namely $f = 0\,\text{mm}^{-1}$ and $f = 0.21\,\text{mm}^{-1}$, are considered, which correspond to the most common spatial frequency range in SFDI[17–19]. According to Figure 4, a deviation in reduced scattering

of more than 5 % exists even at the initial time step and gradually increases to relative errors as large as 25 %.
We attribute the Intralipid layering mostly to gravity induced rise of the largest oil droplets. Moreover, attractive forces between the soybean oil and the Intralipid interface may give an additional contribution to the surface effect, although we make the qualitative finding that layering occurs also if the Intralipid surface is in contact with a glass or epoxy plate or a polyethylene film.
Dilution of Intralipid with distilled water, dilutes both the concentration of oil as well as that of the emulsifying agent lecithin to the same ratio. Therefore, we expect little change in both the overall stability of the emulsion and the size distribution of fat droplets, as was successfully demonstrated by Di Ninni et al.[7]. This is reconfirmed by the fact, that stirring brings back the initial optical properties of Intralipid and reduces the surface layer effect. Furthermore, we conclude from experiments with added absorber, that the studied layering properties of Intralipid are independent from the addition of ink.
All presented quantitative results are based on our two-layer evaluation model which shows very nice agreement with the measured reflectance curves. This model states an approximation for the true and unknown layering in Intralipid. From a physical point of view, a gradual variation of optical properties with depth might be a more realistic assumption, which is substantiated by the obtained change in bottom layer optical properties over time from our two-layer model. Nevertheless, our model performs well in reproducing and quantifying the influence of the surface layer.
Both Intralipid layers where assumed to have the refractive index of distilled water[26,27] in spite of the higher refractive index of soybean oil, which has a maximum weight percentage of 5 % in our samples. According to our analytical model, the possible error in refractive index is too small to significantly influence the fit results. Furthermore, our model based evaluation takes into account the oblique incidence of light projections but does not consider the numerical aperture of the camera objective. Instead, the integral value of the angle resolved reflectance is considered. Monte Carlo simulations with and without consideration of the detector aperture demonstrate a small error in SFD reflectance for high spatial frequencies, which is however time independent and too small to significantly impair our evaluation results.
In the course of one measurement series (one hour), about 100 µm of water evaporated from our experimental vessel with filling height of 70 mm. This evaporation loss has insignificant effect on the overall Intralipid concentration and is accounted for by repeated adjustment of the sample height.

V. VERIFICATION BY SPATIALLY RESOLVED REFLECTANCE

In the following, a spatially resolved reflectance (SRR) setup is used for experimental verification of the Intralipid layering properties. This setup was described earlier[28,29] and is used to similarly investigate the SRR over a duration of one hour for a water-Intralipid dilution with $\mu_s'(600\,\mathrm{nm}) \approx 4\,\mathrm{mm}^{-1}$. Briefly, this setup uses point like illumination of the sample by imaging a 400 µm source fiber on the sample surface. The exact beam profile with a diameter of about 500 µm and the optical transfer function of the setup are measured and considered in the subsequent evaluation process by convolution of the evaluation theory with the beam profile. The incident wavelength is adjusted to (600 ± 7) nm using a monochromator in combination with a xenon light source. Similar to our SFDI measurement protocol, the sample is prepared shortly before measurement and the SRR is measured every four minutes after initial stirring at the beginning of the time series.
Figure 5 compares the obtained SRR for the investi-

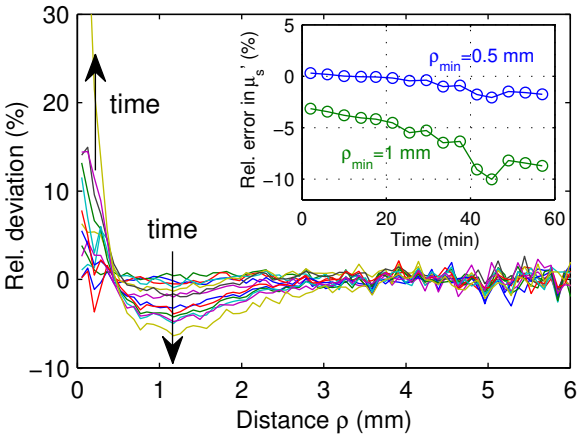

FIG. 5. Relative deviation of the time dependent SRR from the initial reflectance curve captured directly after stirring. Subsequent curves are separated by four minutes and follow a systematic transformation over time. This change gives rise to measurement errors in μ_s', dependent on the minimum evaluation distance ρ_{min} (inset).

gated time series and displays the relative deviation of each measurement from the initial measurement two minutes after stirring. As indicated by the arrows, the given curves change continuously over time, similar to our observations in Figure 2 for SFDI. The signal rises at small distances, drops for distances between 0.5 mm and 4 mm and stays constant at larger distances. This can be attributed to the time-dependent formation of the surface layer. The change follows a clear trend although some irregular steps occur, indicating that the surface layer is inhomogeneous and non-static. Especially the reflectance values at small distances show strong sensitivity to sur-

face inhomogeneities and surface flow.

Figure 6 compares the normalized SRR for Intralipid

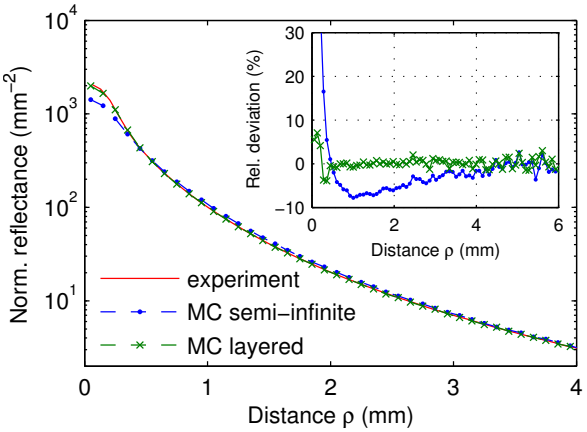

FIG. 6. Comparison of the measured Intralipid SRR for $\mu_s' \approx 4\,\mathrm{mm}^{-1}$ to that of two Monte Carlo simulations assuming either a semi-infinite or a layered Intralipid geometry. The inset shows the relative deviation of the experimental curve from the two simulations and thereby confirms the validity of the layered model.

after 53 minutes to the results of two Monte Carlo (MC) simulations. For qualitative analysis of the surface layer effect, the two Monte Carlo simulations emulate the experimental geometry and assume a semi-infinite and a layered sample geometry, respectively. For the semi-infinite geometry the optical properties of the phantom are set to $\mu_s' = 4\,\mathrm{mm}^{-1}$, $\mu_a = 0.004\,\mathrm{mm}^{-1}$ and $n = 1.33$ in order to approximate the optical properties of the measured Intralipid emulsion. For the layered simulation a thin layer is assumed on top with the surface layer properties obtained from SFDI as given in Figure 3 ($\mu_s'(1) = 10.7\,\mathrm{mm}^{-1}$ and $d = 42.7\,\mu\mathrm{m}$). The remaining parameters of the upper layer are chosen equal to those of the lower layer, and in both simulations the Intralipid scattering phase function and the illumination beam profile of the setup are considered. Figure 6 displays clear differences in the SRR at small distances, when comparing the experimental data to that of the semi-infinite simulation. The relative deviation of the two curves is given in the inset of Figure 6 and resembles that of Figure 5. In contrast, we find good agreement when comparing the layered simulation to the experimental data, which confirms the layer properties measured by SFDI. For small distances a slight error appears which we attribute to inhomogeneities of the surface layer (see inset of Fig. 6).

In the next step, we make use of our experimental SFDI results for the Intralipid layer to theoretically investigate the errors in the optical properties for SRR measurements. To this end, we perform 15 Monte Carlo simulations which correspond to a single time series of one hour. Thereby, we assume a layered medium with the time dependent effective layer thickness as determined by the SFDI approach for $\mu_s' \approx 4\,\mathrm{mm}^{-1}$ (setting $\mu_s'(2) = 4\,\mathrm{mm}^{-1}$ and $\mu_a(1) = \mu_a(2) = 0.004\,\mathrm{mm}^{-1}$). Then, we use a Levenberg-Marquardt algorithm together with the single Monte Carlo method[30] assuming a semi-infinite geometry to fit the Monte Carlo reflectance data. Having the shape of the deviation curve between the layered and the semi-infinite medium in mind (see inset of Fig. 6) it is clear that the errors of the retrieved fit parameters strongly depend on the minimum radial evaluation distance ρ_{min} considered in the fit procedure. The standard fit procedure which we usually use is to fit twice, starting first at a distance of 1 mm and using the resulting μ_s' for a second fit with a start distance of the beam radius plus $1/\mu_s'$. The curve in each fit is evaluated either up to the distance of 23 mm or, if the curve is steep, to a distance where the reflectance has dropped by three orders of magnitude with respect to the starting distance. The latter constraint avoids fitting of noisy data. As only the relative decline of the reflectance is fitted, a multiplicative factor is considered in the fit.

In the inset of Figure 5, relative errors of μ_s' resulting from the fit procedure for two different start distances ρ_{min} are shown. For the start distance of $\rho_{min} = 0.5\,\mathrm{mm}$ we observe relatively small deviation of the reduced scattering coefficient. Even for long times, the error does not exceed 3 %. Also the error in μ_a (not shown) is relatively low and maintains below 5 % for all times considered. This can be explained by the deviation in SRR between measurement and theory, which is positive for small distances and negative for intermediate distances thereby compensating the error of the fit. For the fitting with $\rho_{min} = 1\,\mathrm{mm}$, the obtained errors are much larger and increase from 3 % (initial time) to as much as 10 % after one hour of standstill. At the same time the relative error in μ_a increases from 15 % (initial time) to 35 % (data not shown). In consequence, the errors associated with the Intralipid surface layer can potentially be very large and are strongly dependent on the starting distance ρ_{min}. It should be noted, that the obtained errors in μ_s' given in the inset of Figure 5 are based on our two-layer evaluation model with the additional assumption of constant optical properties of the bottom layer. Larger errors are expected to occur especially at longer times, when also considering this temporal variation of the bottom layer.

VI. CONCLUSION

Intralipid has become one of the most widely used reference materials for diffuse optical imaging technologies. Both the time series of experiments on Intralipid and our use of a two-layer analytical evaluation model reveal the formation of a highly scattering layer on the surface of Intralipid emulsions. This layer seems to be restricted to the upper surface while not being observed on side walls. We find the thickness of this layer to be in the micrometer range and to gradually increase over one hour after stirring of the emulsion. When using Intralipid as a reference material assuming homogeneous phantom prop-

erties, the surface layer can give rise to a measurement error. This error strongly depends on the measurement modality and its corresponding surface sensitivity. Principally, the error can distort the comparison between different measurement techniques.

For SFDI, the obtained errors depend on the considered spatial frequency range and increase for higher spatial frequencies. For typical spatial frequencies, we quantify the error in μ_s' to about 7 % even shortly after stirring of the emulsion. Without repeated stirring of the phantom, this relative error rises to about 25 % within the time of one hour.

SRR measurements relate to the Fourier transform of the SFDI signal and have therefore the same sensitivity to the Intralipid surface layer and potentially produce the same errors in μ_a and μ_s'. Disregard of reflectance values at very short distances can strongly reduce this sensitivity[4]. Depending on the minimal evaluation distance, typical errors in μ_s' are found to lie between 0 % and 3 % directly after stirring and can potentially increase to about 10 % after one hour of standstill.

In contrast, Monte Carlo simulations of fiber based time resolved reflectance reveal almost complete insensitivity to the surface layer, if the previously derived effective layer thicknesses are considered. For source detector separations larger than 6 mm, the obtained deviation in μ_s' is below one percent even after one hour of standstill. This is due to the exclusive consideration of long propagation times of most time resolved approaches. Therefore, both time resolved measurements in general and fiber based measurements with large source detector separations or with the fibers deeply immersed in the emulsion seem to be barely affected by the surface layer.

In conclusion, we do not generally question the merits of Intralipid as a calibration or reference material, but want to raise awareness of the potentially large errors related to the Intralipid layering for surface sensitive techniques. Furthermore, we strongly recommend the avoidance of long standing times of Intralipid before measurements in order to minimize the surface layer induced perturbation.

We have not yet used our model for liquid phantoms other than Intralipid, but assume comparable effects for milk and similar oil-in-water emulsions.

ACKNOWLEDGMENTS

We express our thanks to Fresenius Kabi for the provision of Intralipid and acknowledge the support by the Richard and Annemarie Wolf Foundation, Knittlingen, Germany.

[1]F. Martelli and G. Zaccanti, "Calibration of scattering and absorption properties of a liquid diffusive medium at NIR wavelengths. CW method," *Opt. Express* **15**(2), 486-500 (2007).

[2]H. J. van Staveren et al., "Light scattering in Intralipid-10% in the wavelength range of 400-1100 nm," *Appl. Opt.* **30**(31), 4507-4514 (1991).

[3]S. T. Flock et al., "Optical Properties of Intralipid: A Phantom Medium for Light Propagation Studies," *Lasers Surg. Med.* **12**(5), 510-519 (1992).

[4]L. Spinelli et al., "Determination of reference values for optical properties of liquid phantoms based on Intralipid and India ink," *Biomed. Opt. Express* **5**(7), 2037-2053 (2014).

[5]I. Driver et al., "The optical properties of aqueous suspensions of Intralipid, a fat emulsion," *Phys. Med. Biol.* **34**(12), 1927-1930 (1989).

[6]A. Giusto et al., "Optical properties of high-density dispersions of particles: application to Intralipid solutions," *Appl. Opt.* **42**(21), 4375-4380 (2003).

[7]P. Di Ninni, F. Martelli and G. Zaccanti "Effect of dependent scattering on the optical properties of Intralipid tissue phantoms," *Biomed. Opt. Express* **2**(8), 2265-2278 (2011).

[8]B. Aernouts et al., "Dependent scattering in Intralipid phantoms in the 600-1850 nm range," *Opt. Express* **22**(5), 6086-608 (2014).

[9]S. C. Kanick et al., "Scattering phase function spectrum makes reflectance spectrum measured from Intralipid phantoms and tissue sensitive to the device detection geometry," *Biomed. Opt. Express* **3**(5), 1086-1100 (2012).

[10]R. Michels, F. Foschum and A. Kienle, "Optical Properties of fat emulsions," *Opt. Express* **16**(8), 5907-5925 (2008).

[11]X. Wen et al., "Controlling the scattering of Intralipid by using optical clearing agents," *Phys. Med. Biol.* **54**(22), 6917-6930 (2009).

[12]B. Cletus et al., "Temperature-dependent optical properties of Intralipid measured with frequency-domain photon-migration spectroscopy," *J. Biomed. Opt.* **15**(1), 017003 (2010).

[13]P. Di Ninni, F. Martelli and G. Zaccanti, "Intralipid: towards a diffusive reference standard for optical tissue phantoms," *Phys. Med. Biol.* **56**(2), N21-N28 (2011).

[14]B. Aernouts et al., "Supercontinuum laser based optical characterization of Intralipid phantoms in the 500-2250 nm range," *Opt. Express* **21**(26), 32450-32467 (2013).

[15]P. Rowe et al., "Thermal Stability of Intralipid Optical Phantoms," *Appl. Spectrosc.* **67**(8), 993-996 (2013).

[16]N. Dögnitz and G. Wagnières, "Determination of Tissue Optical Properties by Steady-State Spatial Frequency-Domain Reflectometry," *Lasers in Medical Science* **13**, 55-65 (1998).

[17]D. J. Cuccia et al., "Modulated imaging: quantitative analysis and tomography of turbid media in the spatial-frequency domain," *Opt. Lett.* **30**(11), 1354-1356 (2005).

[18]J. R. Weber et al., "Noncontact imaging of absorption and scattering in layered tissue using spatially modulated structured light," *J. Appl. Phys.* **105**, 102028 (2009).

[19]D. J. Cuccia et al., "Quantitation and mapping of tissue optical properties using modulated imaging," *J. Biomed. Opt.* **14**(2), 024012 (2009).

[20]R. B. Saager, D. J. Cuccia and A. J. Durkin, "Determination of optical properties of turbid media spanning visible and near-infrared regimes via spatially modulated quantitative spectroscopy," *J. Biomed. Opt.* **15**(1), 017012 (2010).

[21]A. M. Laughney et al., "System analysis of spatial frequency domain imaging for quantitative mapping of surgically resected breast tissues," *J. Biomed. Opt.* **18**(3), 036012 (2013).

[22]A. Liemert and A. Kienle, "Spatially modulated light source obliquely incident on a semi-infinite scattering medium," *Opt. Lett.* **37**(19), 4158-4160 (2012).

[23]A. Liemert and A. Kienle, "Exact and efficient solution of the radiative transport equation for the semi-infinite medium," *Scientific Reports* **3**, 2018 (2013).

[24]N. Bodenschatz et al., "Sources of errors in spatial frequency domain imaging of scattering media," *J. Biomed. Opt.* **19**(7), 071405 (2014).

[25]F. Foschum and A. Kienle, "Optimized goniometer for determination of the scattering phase function of suspended particles: simulations and measurements," *J. Biomed. Opt.* **18**(8), 085002 (2013).

[26]M. Daimon and A. Masumur, "Measurement of the refractive index of distilled water from the near-infrared region to the ultraviolet region," *Appl. Opt.* **46**(18), 3811-3820 (2007).
[27]J. Lai et al., "Experimental measurement of the refractive index of biological tissues by total internal reflection," *Appl. Opt.* **44**(10), 1845-1849 (2005).
[28]F. Foschum, M. Jäger and A. Kienle, "Fully automated spatially resolved reflectance spectrometer for the determination of the absorption and scattering in turbid media," *Rev. Sci. Instrum.* **82**(10), 103104 (2011).
[29]F. Foschum and A. Kienle, "Broadband absorption spectroscopy of turbid media using a dual step steady-state method," *J. Biomed. Opt.* **17**(3), 037009 (2012).
[30]A. Kienle and M. S. Patterson, "Determination of the Optical Properties of Turbid Media from a Single Monte Carlo Simulation," *Phys. Med. Biol.* **41**, 2221-2227 (1996).